

# MOVEFM-R: ADVANCING MOBILITY FOUNDATION MODELS VIA LANGUAGE-DRIVEN SEMANTIC REASONING

006 **Anonymous authors**

007 Paper under double-blind review

## ABSTRACT

013 Mobility Foundation Models (MFMs) have advanced the modeling of human  
 014 movement patterns, yet they face a ceiling due to limitations in data scale and  
 015 semantic understanding. While Large Language Models (LLMs) offer powerful  
 016 semantic reasoning, they lack the innate understanding of spatio-temporal  
 017 statistics required for generating physically plausible mobility trajectories. To  
 018 address these gaps, we propose MoveFM-R, a novel framework that unlocks  
 019 the full potential of mobility foundation models by leveraging language-driven  
 020 semantic reasoning capabilities. It tackles two key challenges: the vocabulary  
 021 mismatch between continuous geographic coordinates and discrete language to-  
 022 kens, and the representation gap between the latent vectors of MFMs and the  
 023 semantic world of LLMs. MoveFM-R is built on three core innovations: a se-  
 024 manticly enhanced location encoding to bridge the geography-language gap,  
 025 a progressive curriculum to align the LLM’s reasoning with mobility patterns,  
 026 and an interactive self-reflection mechanism for conditional trajectory genera-  
 027 tion. Extensive experiments demonstrate that MoveFM-R significantly outper-  
 028 forms existing MFM-based and LLM-based baselines. It also shows robust gen-  
 029 eralization in zero-shot settings and excels at generating realistic trajectories from  
 030 natural language instructions. By synthesizing the statistical power of MFMs  
 031 with the deep semantic understanding of LLMs, MoveFM-R pioneers a new  
 032 paradigm that enables a more comprehensive, interpretable, and powerful mod-  
 033 eling of human mobility. The implementation of MoveFM-R is available online  
 034 at <https://anonymous.4open.science/r/MoveFM-R-CDE7/>.

## 1 INTRODUCTION

037 The proliferation of large-scale mobility data from sources like GPS and location-based services has  
 038 revolutionized the modeling of human mobility (Luca et al., 2021; Feng et al., 2018; Yuan et al.,  
 039 2025; Chen et al., 2024), which is a foundational element of human behavior and the engine of  
 040 urban functionality (Gonzalez et al., 2008; Song et al., 2010). The field has witnessed a remarkable  
 041 architectural evolution, progressing from early statistical approaches (Kitamura et al., 1996; Arentze  
 042 et al., 2000; Bowman & Ben-Akiva, 2001) to sophisticated deep learning frameworks (Feng et al.,  
 043 2018; Yang et al., 2022; Yuan et al., 2023; Li et al., 2024; Chu et al., 2023; Zhu et al., 2024a).

044 Inspired by the pursuit of Artificial General Intelligence, the foundation model paradigm has re-  
 045 cently been introduced to the domain of human mobility (Zhou et al., 2024). A new line of research  
 046 has focused on building mobility foundation models (MFM) from scratch (Zhu et al., 2024b; Han  
 047 et al., 2025; Liu et al., 2024b; Long et al., 2025), which have demonstrated remarkable general-  
 048 ization capabilities across a variety of tasks and contexts. Despite their impressive performance, a  
 049 fundamental ceiling remains, stemming from two core issues. On the one hand, the scale of avail-  
 050 able mobility data, though large, is constrained by privacy concerns and collection costs (Kim et al.,  
 051 2020). It is dwarfed by the almost unimaginable scale of web data that fuels LLMs, making it  
 052 difficult to replicate their emergent intelligence from scratch. On the other hand, these models effec-  
 053 tively process geographic coordinates but cannot infer the rich semantic context and human intent  
 that drive these mobility patterns.

054 However, we argue that simply replacing MFM<sub>s</sub> with LLM<sub>s</sub> is not the answer, as LLM<sub>s</sub> are not  
 055 “native speakers” of the continuous, physically-constrained movement; they lack the deep, built-in  
 056 understanding of spatio-temporal statistics and distributions that specialized MFM<sub>s</sub> excel at. Current  
 057 LLM-based models (Shao et al., 2024a; Wang et al., 2024) struggle to ground their reasoning  
 058 in physical reality; they can produce sequences of plausible location types, but these sequences  
 059 are often geographically incoherent or physically infeasible (Koda et al., 2025). The optimal path  
 060 forward is therefore synthesis, not replacement. Building on this premise, our work leverages the  
 061 unique semantic reasoning of LLM<sub>s</sub> to fully unlock the potential of MFM<sub>s</sub>, thereby addressing  
 062 their core limitation in semantic understanding. Furthermore, this paradigm enhances usability, as  
 063 natural language provides a more intuitive and expressive interface for guiding the generation pro-  
 064 cess (Reynolds & McDonell, 2021). For example, the instruction can be like “please generate xxx”.

065 This proposed synthesis, while promising, faces two fundamental challenges. The first is a funda-  
 066 mental vocabulary mismatch. Natural language processing benefits from a finite, shared vocabulary,  
 067 whereas mobility unfolds across a near-infinite and continuous set of locations. Simply discretizing  
 068 coordinates leads to an explosive vocabulary size and loss of precision (Chen et al., 2025). Sec-  
 069 ond, a significant representation gap exists between the two modalities. An MFM’s understanding  
 070 of mobility is expressed through latent vectors that capture the statistical and geometric patterns of  
 071 movement (Hashemi & Zufle, 2025). These representations, however, are not directly interpretable  
 072 by an LLM, which reasons about the world through the lens of human language and semantics (Singh  
 073 et al., 2024).

074 To address these challenges, we propose MoveFM-R, which unifies the mobility understanding of  
 075 MFM<sub>s</sub> with the semantic understanding and reasoning capabilities of LLM<sub>s</sub>. Its design philosophy  
 076 is to bridge the mismatch between continuous trajectories and discrete language, making it easier  
 077 for LLM<sub>s</sub> to understand the spatiotemporal features of MFM trajectories. First, MoveFM-R intro-  
 078 duces semantically enhanced location encoding to discretize continuous coordinates into a set of  
 079 compact, interpretable tokens, alleviating the vocabulary explosion problem and embedding geo-  
 080 graphic semantics in a form that LLM<sub>s</sub> can understand. Second, the description-to-summarization  
 081 process gradually integrates LLM with movement representation generated by MFM, transitioning  
 082 from fine-grained natural language trajectory descriptions to higher-level summaries, thereby en-  
 083 hancing its understanding of mobility behaviors. Finally, a self-reflective reinforcement learning  
 084 strategy iteratively improves the generated trajectories under spatiotemporal constraints, ensuring  
 085 their plausibility and adaptability in diverse scenarios. These designs collectively address core chal-  
 086 lenges, enabling MoveFM-R to seamlessly integrate statistical modeling of human movement with  
 087 semantic reasoning. Our key contributions are summarized as follows:

- 088 • We pioneer a novel paradigm to synthesize the statistical modeling capabilities of MFM<sub>s</sub> with the  
 089 powerful semantic reasoning of LLM<sub>s</sub>, enabling a more comprehensive mobility modeling.
- 090 • We propose MoveFM-R, a framework built on three core innovations: a semantic location en-  
 091 coding to bridge the geography-language gap, a progressive curriculum to align the LLM with  
 092 mobility patterns, and an interactive self-reflection mechanism for conditional generation.
- 093 • We demonstrate state-of-the-art performance on mobility prediction and generation through ex-  
 094 tensive experiments, showing significant improvements over MFM and LLM baselines, robust  
 095 zero-shot generalization, and high-fidelity generation from natural language instructions.

## 097 2 RELATED WORKS

### 100 2.1 BUILDING MOBILITY FOUNDATIONAL MODELS FROM SCRATCH

101 The availability of large-scale trajectory data has facilitated the development of foundational mod-  
 102 els for human mobility. Early work, such as the Pretrained Mobility Transformer (PMT) (Wu  
 103 et al., 2024), demonstrated that large-scale pre-training can capture transferable, region-independent  
 104 movement patterns. Subsequent research has expanded this paradigm, including enhancing cross-  
 105 city transfer capabilities (Kang, 2025), exploring generative frameworks such as diffusion mod-  
 106 els (Chu et al., 2023), and leveraging mixture-of-experts (MoE) architectures for improved scalabil-  
 107 ity (Zhu et al., 2024b; Liu et al., 2024b; Shi et al., 2024; Han et al., 2025). Despite their success in  
 108 modeling statistical patterns, these models operate on coordinate and sequence-based language and

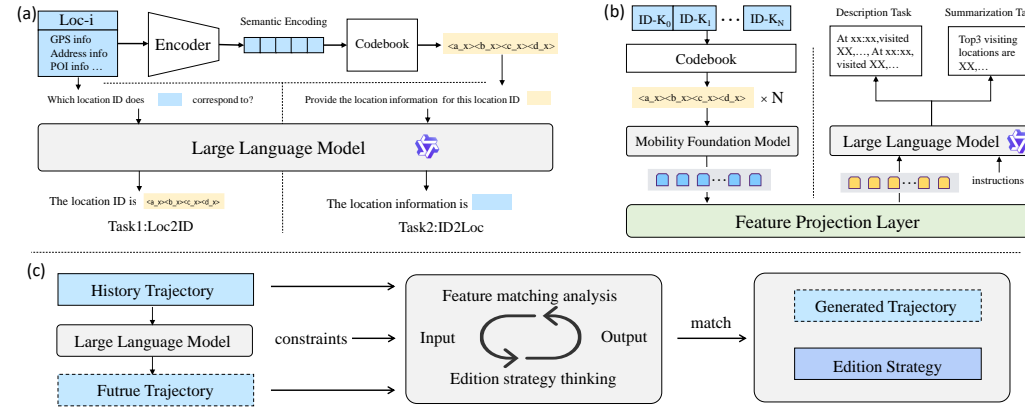


Figure 1: The framework of MoveFM-R. (a) Semantic enhanced location encoding, (b) Mobility understanding from description to summarization, (c) Interactive mobility generation

lack inherent mechanisms for understanding high-level semantics and human intent. This fundamentally limits their reasoning capabilities and motivates the integration of large language models.

## 2.2 LLM-BASED MOBILITY MODELING

Recently, researchers have explored the application of large language models (LLMs) to the mobility domain. Through specialized codebooks or sequence reprogramming (Gong et al., 2024; Chen et al., 2025; Chib & Singh, 2024), continuous trajectories are aligned with the discrete input space of the LLM. On the generative side, researchers have encouraged LLMs to simulate human decision-making processes (Shao et al., 2024a) or act as urban agents to generate trajectories (Wang et al., 2024; Ju et al., 2025). Another approach is to enrich the original trajectories with semantic attributes, such as points of interest (POIs) or activities, to improve model performance (Luo et al., 2024; Liu et al., 2024a; Lan et al., 2024). While these studies successfully incorporate semantic knowledge into mobility modeling, they must reduce continuous trajectories to discrete sequences of symbols in order to make spatiotemporal data digestible to LLMs. This process typically sacrifices geometric accuracy and can produce trajectories that are semantically plausible but geographically incoherent or physically unfeasible. Our research project, MoveFM-R, directly addresses this fundamental challenge by tightly integrating the semantic reasoning capabilities of LLMs with the statistical fidelity of a dedicated mobility encoder, aiming to achieve the best of both worlds.

## 3 METHODOLOGY

To bridge the gap between the statistical power of MFM and the semantic reasoning of LLMs, we propose MoveFM-R. As illustrated in Figure 1, MoveFM-R progressively integrates mobility patterns with the LLM via three core stages: **(a) Semantically Enhanced Location Encoding**, which translates complex geographic location information into a discrete, semantically rich vocabulary for the LLM; **(b) Mobility Understanding from Description to Summarization**, which enables the LLM to comprehend spatiotemporal patterns through a curriculum progression; and **(c) Interactive Mobility Generation**, which empowers the LLM to iteratively refine and generate realistic trajectories under specified instruction constraints.

### 3.1 SEMANTIC ENHANCED LOCATION ENCODING

LLMs inherently lack an understanding of raw geographic coordinates. To address this, we transform discrete locations into a semantically rich vocabulary by discretizing a high-dimensional geographic semantic space (rather than the raw coordinate space). This core design captures the functional and contextual essence of locations. Furthermore, because the language used to describe geographic concepts is largely universal, this semantics-first approach naturally creates a unified codebook that generalizes across different cities. This process involves two stages: (i) Universal Codebook Construction; and (ii) Codebook Alignment with LLM.

162 3.1.1 UNIVERSAL CODEBOOK CONSTRUCTION  
163

164 Our approach begins by establishing a common vocabulary that adheres to a semantics-first principle.  
165 To achieve this, we first compile a comprehensive semantic profile for each location within  
166 a large-scale, multi-city dataset. Rather than relying solely on coordinates, each profile aggregates  
167 diverse textual attributes, including street addresses and 34 types of nearby Points of Interest (POIs),  
168 which are sourced from OpenStreetMap (OSM). These rich, descriptive profiles are then encoded  
169 into high-dimensional semantic vectors using a pre-trained text encoder (Zhang et al., 2025). For  
170 detailed information about textual attributes profile, please refer to the appendix B.  
171

172 The next step is to discretize these vectors into a compact and structured vocabulary. To achieve this,  
173 we employ a Residual Quantized Variational Autoencoder (RQ-VAE) (Lee et al., 2022), a powerful  
174 technique for high-fidelity vector quantization. The RQ-VAE performs hierarchical quantization,  
175 decomposing each semantic vector into a sequence of discrete codewords in a cascaded manner.  
176

177 Formally, given an input semantic vector  $E = r_0 \in \mathbb{R}^d$ , the process iteratively quantizes a residual  
178 vector at each of the  $N$  layers. At the  $n$ -th layer, a codeword vector  $v_{c_n}^n$  is selected from the layer's  
179 codebook  $\mathcal{C}^n$  as the nearest neighbor to the current input residual  $r_n$ :

$$178 \quad v_{c_n}^n = \arg \min_{v \in \mathcal{C}^n} \|r_n - v\|_2^2, \quad (1)$$

180 where the residual for the next layer is calculated as  $r_{n+1} = r_n - v_{c_n}^n$ . This decomposes the original  
181 vector  $E$  into a sequence of indices  $\{c_1, c_2, \dots, c_N\}$ , which serves as its discrete representation.  
182

183 To optimize the codebook, we employ two complementary losses. The residual quantization loss,  
184  $\mathcal{L}_{\text{RQ}}$ , encourages each codebook to accurately represent the input residuals:  
185

$$186 \quad \mathcal{L}_{\text{RQ}} = \sum_{n=1}^N (\|\text{sg}[r_n] - v_{c_n}^n\|_2^2 + \alpha \|r_n - \text{sg}[v_{c_n}^n]\|_2^2), \quad (2)$$

187 where  $\text{sg}[\cdot]$  is the stop-gradient operator, and  $\alpha$  is a balancing hyperparameter. The first term  
188 updates the codewords to match the residuals, while the second aligns the residuals with the se-  
189 lected codewords. Additionally, a reconstruction loss  $\mathcal{L}_{\text{rec}}$  ensures that the sum of quantized vectors,  
190  $\hat{E} = \sum_{n=1}^N v_{c_n}^n$ , remains a faithful representation of the original vector  $E$ :  
191

$$192 \quad \mathcal{L}_{\text{rec}} = \|E - \text{MLP}(\hat{E})\|_2^2. \quad (3)$$

193 The overall training objective is  $\mathcal{L} = \mathcal{L}_{\text{rec}} + \mathcal{L}_{\text{RQ}}$ .  
194

195 In contrast to previous codebook training methods (Chen et al., 2025) using small, single-city data  
196 (often containing only a few thousand locations), training on our large-scale, multi-city dataset of  
197 millions of locations enables the model to learn a robust and general mapping from abstract semantic  
198 concepts to concrete tokens. This process results in a transferable, general vocabulary, laying the  
199 foundation for the model's generalization capabilities.  
200

201 3.1.2 CODEBOOK ALIGNMENT WITH LLM  
202

203 To integrate the new, semantically ungrounded tokens from our geographic codebook into the LLM,  
204 we propose a two-stage alignment methodology. This process first optimizes the static embeddings  
205 of the tokens and subsequently fine-tunes the LLM to comprehend their contextual usage.  
206

207 **Stage 1: Optimizing Initial Token Embeddings.** To avoid a semantically void random initial-  
208 ization, we first set the initial embedding of each new token,  $e_t^{(0)}$ , to the mean of its constituent  
209 subword embeddings from the LLM's vocabulary. However, this serves only as a coarse approxi-  
210 mation. To refine it, we formulate a composite loss function that aligns the new token embeddings  
211 with their original semantic space. For a given location ID, represented by the codeword sequence  
212  $\{t_{i_1}, \dots, t_{i_k}\}$ , we compute their average embedding  $z$  and project it via a linear layer to obtain  
213  $\hat{y} = \text{Linear}(z)$ . The alignment is optimized with the following loss:  
214

$$215 \quad \mathcal{L}_{\text{align}} = \mathcal{L}_{\text{main}} + \lambda_{\text{prior}} \mathcal{L}_{\text{prior}} + \lambda_{\text{coh}} \mathcal{L}_{\text{coh}}. \quad (4)$$

216 Here,  $\mathcal{L}_{\text{main}}$  is a cosine similarity loss that aligns the projected embedding  $\hat{y}$  with the original pre-  
217 quantization semantic vector  $y$ . This loss is regularized by two terms:  $\mathcal{L}_{\text{prior}}$  maintains stability by

penalizing deviation from the initial embeddings, and  $\mathcal{L}_{\text{coh}}$  leverages Pointwise Mutual Information (PMI) (Church & Hanks, 1990) to enforce similar representations for geographically co-occurring locations.

$$\mathcal{L}_{\text{main}} = \mathbb{E} \left[ \max(0, 1 - \cos(\hat{y}, y)) \right], \mathcal{L}_{\text{prior}} = \frac{1}{M} \sum_{t \in \mathcal{N}} \|e_t - e_t^{(0)}\|_2^2, \mathcal{L}_{\text{coh}} = \frac{1}{|\mathcal{E}|} \sum_{(t, u)} \text{PMI}(t, u) \|e_t - e_u\|_2^2. \quad (5)$$

Upon completion, the optimized embeddings are integrated into the LLM’s vocabulary matrix, establishing a robust semantic foundation for the next stage.

**Stage 2: Contextual Fine-tuning via Bidirectional Instruction-Tuning.** With semantically meaningful embeddings established, we fine-tune the LLM through a supervised, bidirectional instruction-tuning task, designed to enable it to understand and apply these tokens in context. The process has two complementary objectives:

1. **Interpretation (ID-to-Description):** Given a Location ID, the model is trained to generate its corresponding geographic description. This enables the LLM to interpret the semantics of specialized tokens.
2. **Retrieval (Description-to-ID):** Conversely, given a geographic description, the model must generate the correct Location ID. This enables the LLM to retrieve and apply the symbolic tokens as needed.

This bidirectional training ensures the model can proficiently map between symbolic identifiers and natural language, bridging the final gap. Detailed prompt designs are provided in Appendix D.

### 3.2 MOBILITY UNDERSTANDING FROM DESCRIPTION TO SUMMARIZATION

While the semantic encoding in Section 3.2 provides the LLM with a mobility "vocabulary", genuine comprehension requires mastering the "grammar" of human movement—the ability to infer underlying spatiotemporal patterns from an MFM’s latent trajectory sequence. To install this capability, we introduce a mobility-aware alignment curriculum. As illustrated in Figure 1(b), this strategy systematically guides the LLM from perceiving factual events to reasoning about abstract patterns. The curriculum unfolds in two progressive stages:

1. **Low-level mobility trajectory description task:** The LLM translates the MFM’s latent sequence into a trajectory description of facts (e.g., "At time  $t$ , the user visited location  $l$ .)
2. **High-level spatiotemporal pattern summarization task:** The LLM learns to reason about the sequence encoding to infer abstract travel patterns, such as identifying frequently visited locations and modeling the temporal evolution of movement probabilities.

Crucially, this curriculum is not merely a pre-training understanding phase; it is architecturally integrated into the model’s decision-making process for downstream applications. We formulate prediction and generation as a conditional, multi-part objective where the LLM is prompted to first output the high-level spatiotemporal feature summary before providing the final prediction or generation. This design choice is critical: it establishes a coherent "**understanding → prediction | generation**" reasoning chain. By forcing the model to articulate its reasoning first, we provide a strong inductive bias that compels it to base its predictions on inferred spatiotemporal patterns rather than on superficial sequence correlations. Detailed prompt designs are provided in the Appendix D.

**Training loss.** The aforementioned tasks of understanding, prediction, and generation are optimized through supervised fine-tuning. Given an input trajectory sequence  $X_{\text{seq}}$ , it is first processed by the MFM encoder, denoted as  $g_\phi$ . The resulting representation is then projected into the LLM’s input embedding space via a lightweight MLP, yielding the final conditioning hidden state  $H_{\text{seq}} = \text{MLP}(g_\phi(X_{\text{seq}}))$ . Conditioned on this mobility representation  $H_{\text{seq}}$  and a corresponding text instruction  $X_{\text{Ins}}$ , the LLM is trained to autoregressively generate the target text output  $y = (y_1, y_2, \dots, y_N)$ . The model’s parameters  $\theta$  are optimized by minimizing the negative log-likelihood of the ground-truth sequence. The loss function  $\mathcal{L}$  is defined as:

$$\mathcal{L} = -\frac{1}{N} \sum_{t=1}^N \log P_\theta(y_t | y_{<t}, X_{\text{Ins}}, X_{\text{seq}}) \quad (6)$$

270 3.3 INTERACTIVE MOBILITY GENERATION  
271

272 While mobility foundational models excel at capturing historical patterns, their architecture inher-  
273 ently lacks the flexibility to generate trajectories under arbitrary, open-ended scenarios. Integrating  
274 LLMs offers a powerful new avenue to address this limitation, enabling the generation of trajectories  
275 that conform to diverse, language-specified conditions. The core challenge of this task lies in the  
276 dual objective of strictly adhering to the scenario’s explicit spatiotemporal constraints while main-  
277 taining high fidelity to the user’s ingrained behavioral patterns. To resolve this tension, we introduce  
278 a Self-Reflective Reasoning strategy, which begins with a baseline generated trajectory derived from  
279 user history and applies the minimal necessary edits to satisfy the new constraints, ensuring the final  
280 trajectory is both scenario-compliant and behaviorally consistent.

281 3.3.1 SELF-REFLECTIVE REASONING  
282

283 Our **Self-Reflective Reasoning** operationalizes the “minimal edits” principle through a structured,  
284 iterative process, as illustrated in Figure 1(c). Instead of generating a trajectory in a single pass, the  
285 model engages in a deterministic loop of generation, critique, and refinement. The process unfolds  
286 as follows:

- 287 1. **Baseline Generation.** The model first generates an initial future trajectory based on the user’s  
288 historical data. This serves as a critical “zero-scenario” baseline, a starting point that is by  
289 definition fully consistent with the user’s established spatiotemporal patterns.
- 290 2. **Iterative Refinement.** The model then enters a refinement loop. It compares the current tra-  
291 jectory against the explicit spatiotemporal constraints of the target scenario. If any statistical  
292 mismatches are detected, the model proposes a targeted edit. After applying the edit, the modi-  
293 fied trajectory is re-evaluated.
- 294 3. **Termination.** This loop continues until the trajectory fully satisfies all scenario constraints.  
295 Upon reaching this self-consistent state, the model outputs the final edited trajectory, along with  
296 a structured summary of the edits and their justifications.

297 We address the dual objectives outlined previously through a simple yet powerful heuristic: explic-  
298 itely instructing the model to seek a solution requiring the fewest number of edits, ensuring that the  
299 final output is a true synthesis, rather than a completely new, unrelated behavior. To guide the model  
300 in planning edits, we define a discrete action space containing three permissible edit operations: (i)  
301 adding a trajectory point, (ii) deleting a trajectory point, or (iii) modifying the time and/or position  
302 of an existing point.

304 3.3.2 REWARD MODELING FOR RL TRAINING  
305

306 We implement iterative trajectory reasoning using Group Relative Policy Optimization  
307 (GRPO) (Shao et al., 2024b). Compared with PPO (Schulman et al., 2017), GRPO eliminates  
308 the need for a separately trained value function by using group-relative rewards to compute advan-  
309 tages, significantly reducing memory and computational overhead, which better suits LLM tasks. The  
310 model is trained to follow the reasoning template detailed in Table 1.

311 Table 1: Template for Self-Reflective Reasoning with GRPO

312 Please answer the following questions step by step. You need to think and reason before  
313 answering, outputting your reasoning process between `<think>` and `</think>`, and pro-  
314 viding your final answer between `<answer>` and `</answer>`.

315 **Input:** Historical trajectory data, initial generated trajectory, spatiotemporal constraints.

316 **Task:** Modify the initial trajectory data based on the historical data and the spatiotemporal  
317 constraints of the scene. Ensure that the modified trajectory conforms to the given statistical  
318 spatiotemporal characteristics and uses the minimum modification step size.

320 The design of the reward function is guided by a crucial objective: **distributional consistency**.  
321 Unlike common reasoning tasks that target an exact-match (EM) solution, our goal is to generate  
322 trajectories that align with the correct statistical distribution. Consequently, we formulate a re-  
323 ward function based on matching key spatiotemporal statistical properties (e.g., travel probability  
at different time periods, and probability distribution of visited places) rather than the ground-truth

324 trajectory. Let  $\phi(\tau)$  denote the statistical feature of trajectory  $\tau$ . The reward is:  
 325

$$326 \quad R_{\text{distribution}}(\tau) = \sum_{k=1}^K \mathbf{1}[\phi_k(\tau) = \phi_k(\tau^*)], \quad (7)$$

327

328 where  $\tau^*$  is the ground truth trajectory. Each matched feature contributes +1 for the reward. Additionally, to avoid unrealistic length deviations, we penalize discrepancies between generated and  
 329 ground-truth lengths:  
 330

$$331 \quad R_{\text{length}}(\tau) = -\frac{||\tau| - |\tau^*||}{|\tau^*|}. \quad (8)$$

332

333 In summary, the total reward can be expressed as follows:  $R(\tau) = R_{\text{distribution}}(\tau) + R_{\text{length}}(\tau)$ .  
 334

335 In addition, to further ensure training stability, we begin with supervised fine-tuning (SFT) as a cold-  
 336 start phase prior to GRPO training. This initialization allows the model to produce well-structured  
 337 outputs and prevents instability during early reinforcement learning. Therefore, we do not need  
 338 the format-based rewards (e.g., validating the `<think>` and `<answer>` tags), as SFT sufficiently  
 339 enforces adherence to the training template.  
 340

## 341 4 EXPERIMENT

### 342 4.1 EXPERIMENTAL SETUP

343 **Dataset:** We evaluated our approach on four real-world human mobility datasets (Atlanta, Chicago,  
 344 Seattle, and Washington, D.C., USA). The geographic space of each city was discretized into 500-  
 345 meter grid cells, with a minimum temporal granularity of 30 minutes. User trajectories were con-  
 346 structed using a sliding window covering three consecutive days, and trajectories with fewer than five  
 347 trips were discarded to reduce sparsity and noise. And if the trajectory exceeded 145 points, only the  
 348 most recent 145 trajectory points were retained. For each visited location, we combined geographic  
 349 coordinates with semantic information (e.g., points of interest) extracted from OpenStreetMap. We  
 350 take careful measures to ensure that ethical considerations are fully addressed in the use of data.  
 351 Further details on the dataset statistics and preprocessing are provided in the Appendix C.  
 352

353 **Evaluation Metrics:** For **prediction task**, we adopt commonly used metrics, hating rating ( $HR@1$ )  
 354 to evaluate the prediction performance (Han et al., 2025; Chen et al., 2025). For **generation task**, we  
 355 adopt commonly used metrics  $BLEU$ ,  $TVD$ , and  $JSD$  to measure the time and location similarity  
 356 between the generated sequence and the real sequence respectively (Reed et al., 2016; Wang et al.,  
 357 2024). For the more details on all metrics above, please refer to the Appendix E.  
 358

359 **Baselines:** For **prediction task**, we selected DeepMove (Feng et al., 2018), TrajBert (Si et al.,  
 360 2023), GETNext (Yang et al., 2022), TrajFM (Lin et al., 2024), Unitraj (Zhu et al., 2024b), and Traj-  
 361 MoE (Han et al., 2025) as traditional deep learning approaches. Among these, Unitraj and TrajMoE  
 362 are pre-trained foundation sequence methods. For LLM-based prediction approaches, we selected  
 363 Mobility-LLM (Gong et al., 2024) and QT-Mob (Chen et al., 2025). For **generation task**, we se-  
 364 lected two recent diffusion-based approaches, DiffTraj (Zhu et al., 2023) and Marionette (Deng et al.,  
 365 2025) and LLM-enhanced generation approaches, COPB (Shao et al., 2024a) and LLMob (Wang  
 366 et al., 2024). For more details on the above baselines, see the Appendix F.  
 367

368 **Implementation Details:** The experiments were conducted on four NVIDIA A800 40G GPUs,  
 369 using Qwen2.5-7B (Hui et al., 2024) as the backbone network and TrajMOE (Han et al., 2025)  
 370 as the enhanced mobility foundation model. We employed LoRA fine-tuning (Hu et al., 2022)  
 371 and parallel training for acceleration. For the reflective reasoning experiments, we utilized two  
 372 additional NVIDIA A100 80G GPUs with Qwen3-4B (Yang et al., 2025) as the backbone. For more  
 373 experimental details, please refer to the Appendix G.  
 374

### 375 4.2 MOBILITY PREDICTION

376 **Next Location Prediction:** We evaluated the performance of all methods on four benchmark  
 377 datasets. Note that methods supporting cross-city pre-training (e.g., TrajMoE) were trained on a

378  
379 Table 2: Experiment result on prediction task(HR@1).  
380

	DeepMove	GETNext	TrajFM	Unitraj	TrajMoE	Mobility-LLM	QT-Mob	<b>MoveFM-R</b>	Improve
Atlanta	0.171	0.178	0.196	0.210	<u>0.245</u>	0.214	0.240	<b>0.281</b>	+14.7%
Chicago	0.188	0.189	0.212	0.219	<u>0.269</u>	0.218	<u>0.306</u>	<b>0.334</b>	+9.2%
Seattle	0.220	0.227	0.255	0.283	0.309	0.270	<u>0.315</u>	<b>0.368</b>	+16.8%
Washington	0.204	0.197	0.202	0.215	0.265	0.224	<u>0.286</u>	<b>0.328</b>	+14.7%

384  
385 Table 3: Experiment result on zero-shot and few-shot(HR@1).  
386

Method	Atlanta		Chicago		Seattle		Washington	
	zero-shot	few-shot	zero-shot	few-shot	zero-shot	few-shot	zero-shot	few-shot
TrajMoE	0.121	0.151	0.085	0.098	0.146	0.194	0.141	0.168
QT-Mob	<u>0.132</u>	<u>0.203</u>	<u>0.242</u>	<u>0.255</u>	<u>0.218</u>	<u>0.244</u>	<u>0.242</u>	<u>0.271</u>
Ours	<b>0.164</b>	<b>0.264</b>	<b>0.280</b>	<b>0.309</b>	<b>0.262</b>	<b>0.294</b>	<b>0.272</b>	<b>0.292</b>
Improve	+24.24%	+30.05%	+15.70%	+21.18%	+20.18%	+20.49%	+12.40%	+7.75%

393 mixed dataset from all four cities and tested on each city’s dataset to maximize the benefits of  
394 their pre-training. The results, summarized in Table 2, reveal several key observations: First, our  
395 method improves prediction accuracy by over 10% on average across all datasets. And compared  
396 to TrajMoE (selected as the fundamental model for our method), our method, achieves over 20%  
397 improvement, demonstrating its ability to enhance pre-trained fundamental models. Moreover, our  
398 approach outperforms the LLM baseline, which relies solely on plain text input, by an additional  
399 10%, emphasizing the value of spatiotemporal features captured by domain-specific models.

400 **Zero-Shot and Few-Shot Performance** For the zero-shot experiments, we pre-trained the model  
401 on data from three cities and tested it on the remaining cities (treated as novel environments). For  
402 the few-shot experiments, we fine-tuned the model on 500 examples from the remaining cities and  
403 then tested it. The results, presented in Table 3, reveal several key findings. First, our approach  
404 consistently outperforms both the strongest sequence-based and LLM baseline models (TrajMoE, QT-  
405 Mob) in terms of zero-shot and few-shot performance across all four cities, demonstrating robust  
406 generalization to novel environments. Second, the LLM-based approach, QT-MOB, comprehen-  
407 sively outperforms the purely sequence-based model, TrajMoE, highlighting the impressive ability  
408 of language models to transfer knowledge across diverse urban environments. Notably, our ap-  
409 proach achieves zero-shot accuracy in all four cities that surpasses the classic method, DeepMove,  
410 even when the latter is fine-tuned on the full dataset, further emphasizing the strong generalization  
411 capabilities of our method.

### 412 4.3 MOBILITY GENERATION

413 **Unconditional Generation** For gen-  
414 eration tasks, we focus more on the  
415 distribution consistency (fidelity) be-  
416 tween the generated sequences and  
417 the real sequences rather than accu-  
418 racy. We evaluated all methods on  
419 four city datasets, where the task was  
420 to generate a user’s trajectory on the third day based solely on historical data from the previous  
421 two days. The results, presented in Table 4, reveal several key observations. For more details on  
422 indicator calculations, please refer to the appendix E.

423 First, our method achieves state-of-the-art performance across all metrics(*BLEU*, *TVD*, and *JSD*)  
424 for both temporal and location distribution. Second, by leveraging the fundamental mobility model’s  
425 capacity to extract informative features from numerical sequences, our method significantly out-  
426 performs all LLM-based baselines(COPB,LLMob), which highlights the importance of grounding  
427 LLM reasoning in domain-specific representations rather than relying exclusively on textual input.  
428 Furthermore, our method surpasses pure sequence modeling approaches(DiffTraj,Marionette) by  
429 benefiting from the semantic understanding and reasoning capabilities of LLMs. Together, these  
430 findings demonstrate that integrating structured trajectory features with LLM provides consistent  
431 advantages over both traditional architectures and LLM-only methods.

432  
433 Table 4: Performance of unconditional generation.

Method	Time			Location		
	Bleu ↑	TVD ↓	JSD ↓	Bleu ↑	TVD ↓	JSD ↓
DiffTraj	0.387	0.117	0.009	0.076	0.494	0.220
Marionette	0.582	0.082	0.008	0.092	0.346	0.102
COPB	0.426	0.096	0.009	0.084	0.382	0.133
LLMob	0.605	0.085	0.007	0.095	0.323	0.095
<b>Ours</b>	<b>0.628</b>	<b>0.064</b>	<b>0.006</b>	<b>0.136</b>	<b>0.250</b>	<b>0.062</b>

432 **Conditional Generation** We evaluated  
 433 the model’s conditional trajectory  
 434 performance in three  
 435 representative scenarios: (i) **late-**  
 436 **night commuters**, where nighttime  
 437 trips account for over three-quarters  
 438 of all trips; (ii) **users with tempo-**  
 439 **rary travel plans**, such as those mak-  
 440 ing a last-minute decision to visit or  
 441 not visit a place; and (iii) **weekend**  
 442 **users**, where historical sequences cor-  
 443 respond to Thursdays and Fridays, and generated trajectories  
 444 correspond to Saturdays. These scenarios capture diverse travel patterns and provide a comprehensive  
 445 test of scenario-based generation. Detailed division information is available in appendix I.

446 The results (shown in Table 5) show that our approach achieves significant improvements over  
 447 scenario-free generation (represented as ‘w/o SR’) in most scenarios, though the temporal distri-  
 448 butions for users with explicit travel plans and weekend users are slightly inferior. This success  
 449 stems from our self-reflective reasoning, which effectively exploits scenario-specific spatiotemporal  
 450 constraints. For example, it enforces temporal regularity for late-night commuters (improving time)  
 451 and uses the destination as a strong spatial anchor for users with explicit plans (improving space).  
 452 Conversely, the slight temporal decline reveals a challenge with high stochasticity and pattern shift;  
 453 the model struggles to predict highly variable weekend timing from weekday data or when travel  
 454 times are inherently random despite a fixed destination. In such cases, the unconditional model’s  
 455 more generalized distribution proves advantageous.

#### 456 4.4 ABLATION STUDY

457 To validate the effectiveness of each component in our framework, we conducted ablation studies on  
 458 four datasets. We evaluated the model under four settings: (i) without CB (codebook), (ii) without  
 459 RU (representation understanding), (iii) without FM (base model). The results for the prediction  
 460 task are in Table 6, and for the generation task in Table 7. Key observations include:

461 First, removing both the base model and the codebook results in a significant drop in performance,  
 462 highlighting the importance of the spatiotemporal trajectory features and spatial semantics provided  
 463 by the base model and the structured position encoding. Second, removing representation under-  
 464 standing results in a moderately consistent drop in performance on both tasks, highlighting that  
 465 fine-grained feature understanding helps the LLM better exploit spatiotemporal information. This  
 466 effect is slightly more pronounced in the generation task. Overall, these ablation results confirm  
 467 that each component makes a meaningful contribution and that they collectively enhance trajectory  
 468 prediction and generation.

469 Table 6: Results of ablation studies (predic-  
 470 tion).

Method	Atlanta	Chicago	Seattle	Washington
Ours	0.281	0.334	0.368	0.328
w/o CB	0.243	0.310	0.326	0.306
w/o RU	0.270	0.328	0.350	0.314
w/o FM	0.259	0.318	0.337	0.304

471 Table 7: Results of ablation studies (generation).

Method	Time			Location		
	Bleu $\uparrow$	TVD $\downarrow$	JSD $\downarrow$	Bleu $\uparrow$	TVD $\downarrow$	JSD $\downarrow$
Ours	0.628	0.064	0.006	0.136	0.250	0.062
w/o CB	0.598	0.090	0.007	0.112	0.273	0.072
w/o RU	0.613	0.072	0.006	0.108	0.265	0.068
w/o FM	0.594	0.087	0.007	0.108	0.278	0.074

## 472 5 CONCLUSION

473 This research repositions the ultimate goal of human mobility modeling: moving beyond mere pat-  
 474 tern prediction to achieve a genuine understanding of human intent. Our work demonstrates that the  
 475 key to this evolution lies in the thoughtful synthesis of statistically powerful MFM and the deep  
 476 semantic reasoning of LLMs. We have shown that this synergy is not just a theoretical possibility  
 477 but a practical reality, creating models that can interpret the “why” behind the “where”. The value  
 478 of this new paradigm is profound. It unlocks the ability to interact with and steer mobility genera-  
 479 tion through natural language, making sophisticated simulation and analysis accessible to a broader  
 480 range of experts, including urban planners and social scientists.

486  
487  
**ETHICS STATEMENT**

488  
489 We have implemented robust measures to ensure the ethical handling of data throughout this study,  
490 with a focus on privacy, security, and bias mitigation. To protect individual privacy, the trajectory  
491 data underwent a rigorous anonymization process and contains no personally identifiable information  
492 (PII). To further render the re-identification of individuals infeasible, random noise was added  
493 to all location data points, a technique known as location perturbation. All datasets are stored on  
494 secure, encrypted servers with strict access control protocols, limiting access to authorized research  
495 personnel bound by non-disclosure agreements. Furthermore, to proactively address fairness, the  
496 dataset intentionally excludes any demographic or user-specific attributes, such as gender, race, or  
497 age. This design inherently mitigates the risk of our model learning or perpetuating societal biases  
498 related to these characteristics. We believe this research holds the potential for significant positive  
499 societal impact by contributing to a deeper understanding of human mobility for applications in  
500 areas like intelligent urban planning and transportation systems.

501  
502  
**REPRODUCIBILITY STATEMENT**

503 To ensure the reproducibility of our research, we commit to making our work as transparent and  
504 accessible as possible.

- 505 • **Code:** The source code for our proposed model, experimental setup, and evaluation scripts will  
506 be made publicly available in a GitHub repository upon publication of this work. The repository  
507 will include detailed instructions for setting up the environment and running the experiments.
- 508 • **Implementation Details:** Key hyperparameters and architectural choices for our model are de-  
509 scribed in the main paper. A comprehensive list of all hyperparameters, along with details about  
510 the computational environment (hardware, software libraries, and versions), will be provided in  
511 the `README.md` file of our code repository.

512 The implementation of MoveFM-R is available online at [https://anonymous.4open.scie-  
513 nce/r/MoveFM-R-CDE7/](https://anonymous.4open.science/r/MoveFM-R-CDE7/)

514  
515  
**REFERENCES**

516  
517 Theo Arentze, Frank Hofman, Henk Van Mourik, and Harry Timmermans. Albatross: multiagent,  
518 rule-based model of activity pattern decisions. *Transportation Research Record*, 1706(1):136–  
519 144, 2000.

520 John L Bowman and Moshe E Ben-Akiva. Activity-based disaggregate travel demand model system  
521 with activity schedules. *Transportation research part a: policy and practice*, 35(1):1–28, 2001.

522 Wei Chen, Yuxuan Liang, Yuanshao Zhu, Yanchuan Chang, Kang Luo, Haomin Wen, Lei Li, Yanwei  
523 Yu, Qingsong Wen, Chao Chen, et al. Deep learning for trajectory data management and mining:  
524 A survey and beyond. *arXiv preprint arXiv:2403.14151*, 2024.

525 Yile Chen, Yicheng Tao, Yue Jiang, Shuai Liu, Han Yu, and Gao Cong. Enhancing large language  
526 models for mobility analytics with semantic location tokenization. In *Proceedings of the 31st*  
527 *ACM SIGKDD Conference on Knowledge Discovery and Data Mining* V. 2, pp. 262–273, 2025.

528 Pranav Singh Chib and Pravendra Singh. Lg-traj: Llm guided pedestrian trajectory prediction. *arXiv*  
529 *preprint arXiv:2403.08032*, 2024.

530 Chen Chu, Hengcai Zhang, and Feng Lu. Trajgdm: A new trajectory foundation model for simulating  
531 human mobility. In *Proceedings of the 31st ACM International Conference on Advances in*  
532 *Geographic Information Systems*, pp. 1–2, 2023.

533 Kenneth Church and Patrick Hanks. Word association norms, mutual information, and lexicography.  
534 *Computational linguistics*, 16(1):22–29, 1990.

540 Bangchao Deng, Ling Ding, Lianhua Ji, Chunhua Chen, Xin Jing, Bingqing Qu, and Dingqi Yang.  
 541 Marionette: Fine-grained conditional generative modeling of spatiotemporal human trajectory  
 542 data beyond imitation. In *Proceedings of the 31st ACM SIGKDD Conference on Knowledge  
 543 Discovery and Data Mining* V. 2, pp. 463–473, 2025.

544 Jie Feng, Yong Li, Chao Zhang, Funing Sun, Fanchao Meng, Ang Guo, and Depeng Jin. Deepmove:  
 545 Predicting human mobility with attentional recurrent networks. In *Proceedings of the 2018 world  
 546 wide web conference*, pp. 1459–1468, 2018.

547 Letian Gong, Yan Lin, Xinyue Zhang, Yiwen Lu, Xuedi Han, Yichen Liu, Shengnan Guo, Youfang  
 548 Lin, and Huaiyu Wan. Mobility-llm: Learning visiting intentions and travel preference from  
 549 human mobility data with large language models. *Advances in Neural Information Processing  
 550 Systems*, 37:36185–36217, 2024.

552 Marta C Gonzalez, Cesar A Hidalgo, and Albert-Laszlo Barabasi. Understanding individual human  
 553 mobility patterns. *nature*, 453(7196):779–782, 2008.

555 Chonghua Han, Yuan Yuan, Kaiyan Chen, Jingtao Ding, and Yong Li. Trajmo: Spatially-aware  
 556 mixture of experts for unified human mobility modeling. *arXiv preprint arXiv:2505.18670*, 2025.

557 Mohammad Hashemi and Andreas Zufle. From points to places: Towards human mobility-driven  
 558 spatiotemporal foundation models via understanding places. *arXiv preprint arXiv:2506.14570*,  
 559 2025.

560 Edward J Hu, Yelong Shen, Phillip Wallis, Zeyuan Allen-Zhu, Yuanzhi Li, Shean Wang, Lu Wang,  
 561 Weizhu Chen, et al. Lora: Low-rank adaptation of large language models. *ICLR*, 1(2):3, 2022.

563 Binyuan Hui, Jian Yang, Zeyu Cui, Jiaxi Yang, Dayiheng Liu, Lei Zhang, Tianyu Liu, Jiajun Zhang,  
 564 Bowen Yu, Keming Lu, et al. Qwen2. 5-coder technical report. *arXiv preprint arXiv:2409.12186*,  
 565 2024.

566 Chenlu Ju, Jiaxin Liu, Shobhit Sinha, Hao Xue, and Flora Salim. Trajilm: A modular llm-enhanced  
 567 agent-based framework for realistic human trajectory simulation. In *Companion Proceedings of  
 568 the ACM on Web Conference 2025*, pp. 2847–2850, 2025.

569 LIU Kang. From specialized trajectory models to trajectory foundation models: Advancements and  
 570 prospects. *Journal of Geo-information Science*, 27(7):1520, 2025. doi: 10.12082/dqxxkx.2025.2  
 571 50196. URL <https://www.dqxxkx.cn/EN/10.12082/dqxxkx.2025.250196>.

573 Joon-Seok Kim, Hyunjee Jin, Hamdi Kavak, Ovi Chris Rouly, Andrew Crooks, Dieter Pfoser, Carola  
 574 Wenk, and Andreas Züffle. Location-based social network data generation based on patterns of  
 575 life. In *2020 21st IEEE International Conference on Mobile Data Management (MDM)*, pp.  
 576 158–167. IEEE, 2020.

578 Ryuichi Kitamura, Eric I Pas, Clarisse V Lula, T Keith Lawton, and Paul E Benson. The sequenced  
 579 activity mobility simulator (sams): an integrated approach to modeling transportation, land use  
 580 and air quality. *Transportation*, 23(3):267–291, 1996.

581 Miho Koda, Yu Zheng, Ruixian Ma, Mingyang Sun, Devesh Pansare, Fabio Duarte, and Paolo  
 582 Santi. Locationreasoner: Evaluating llms on real-world site selection reasoning. *arXiv preprint  
 583 arXiv:2506.13841*, 2025.

585 Zhengxing Lan, Lingshan Liu, Bo Fan, Yisheng Lv, Yilong Ren, and Zhiyong Cui. Traj-llm: A new  
 586 exploration for empowering trajectory prediction with pre-trained large language models. *IEEE  
 587 Transactions on Intelligent Vehicles*, 2024.

588 Doyup Lee, Chiheon Kim, Saehoon Kim, Minsu Cho, and Wook-Shin Han. Autoregressive image  
 589 generation using residual quantization. In *Proceedings of the IEEE/CVF conference on computer  
 590 vision and pattern recognition*, pp. 11523–11532, 2022.

591 Siyu Li, Toan Tran, Haowen Lin, John Krumm, Cyrus Shahabi, Lingyi Zhao, Khurram Shafique,  
 592 and Li Xiong. Geo-llama: Leveraging llms for human mobility trajectory generation with spa-  
 593 tiotemporal constraints. *arXiv preprint arXiv:2408.13918*, 2024.

594 Yan Lin, Tonglong Wei, Zeyu Zhou, Haomin Wen, Jilin Hu, Shengnan Guo, Youfang Lin, and  
 595 Huaiyu Wan. Trajfm: A vehicle trajectory foundation model for region and task transferability.  
 596 *arXiv preprint arXiv:2408.15251*, 2024.

597 Shuai Liu, Ning Cao, Yile Chen, Yue Jiang, and Gao Cong. nextlocllm: next location prediction  
 598 using llms. *arXiv preprint arXiv:2410.09129*, 2024a.

600 Xu Liu, Juncheng Liu, Gerald Woo, Taha Aksu, Yuxuan Liang, Roger Zimmermann, Chenghao  
 601 Liu, Silvio Savarese, Caiming Xiong, and Doyen Sahoo. Moirai-moe: Empowering time series  
 602 foundation models with sparse mixture of experts. *arXiv preprint arXiv:2410.10469*, 2024b.

603 Qingyue Long, Can Rong, Huandong Wang, and Yong Li. One fits all: General mobility trajectory  
 604 modeling via masked conditional diffusion. *arXiv preprint arXiv:2501.13347*, 2025.

606 Massimiliano Luca, Gianni Barlacchi, Bruno Lepri, and Luca Pappalardo. A survey on deep learning  
 607 for human mobility. *ACM Computing Surveys (CSUR)*, 55(1):1–44, 2021.

608 Yuxiao Luo, Zhongcai Cao, Xin Jin, Kang Liu, and Ling Yin. Deciphering human mobility: In-  
 609 ferring semantics of trajectories with large language models. In *2024 25th IEEE International  
 610 Conference on Mobile Data Management (MDM)*, pp. 289–294. IEEE, 2024.

612 Scott Reed, Zeynep Akata, Xinchen Yan, Lajanugen Logeswaran, Bernt Schiele, and Honglak Lee.  
 613 Generative adversarial text to image synthesis. In *International conference on machine learning*,  
 614 pp. 1060–1069. Pmlr, 2016.

615 Laria Reynolds and Kyle McDonell. Prompt programming for large language models: Beyond  
 616 the few-shot paradigm. In *Extended abstracts of the 2021 CHI conference on human factors in  
 617 computing systems*, pp. 1–7, 2021.

618 John Schulman, Filip Wolski, Prafulla Dhariwal, Alec Radford, and Oleg Klimov. Proximal policy  
 619 optimization algorithms. *arXiv preprint arXiv:1707.06347*, 2017.

621 Chenyang Shao, Fengli Xu, Bingbing Fan, Jingtao Ding, Yuan Yuan, Meng Wang, and Yong Li.  
 622 Chain-of-planned-behaviour workflow elicits few-shot mobility generation in llms. *arXiv preprint  
 623 arXiv:2402.09836*, 2024a.

624 Zhihong Shao, Peiyi Wang, Qihao Zhu, Runxin Xu, Junxiao Song, Xiao Bi, Haowei Zhang,  
 625 Mingchuan Zhang, YK Li, Yang Wu, et al. Deepseekmath: Pushing the limits of mathematical  
 626 reasoning in open language models. *arXiv preprint arXiv:2402.03300*, 2024b.

628 Xiaoming Shi, Shiyu Wang, Yuqi Nie, Dianqi Li, Zhou Ye, Qingsong Wen, and Ming Jin. Time-  
 629 moe: Billion-scale time series foundation models with mixture of experts. *arXiv preprint  
 630 arXiv:2409.16040*, 2024.

631 Junjun Si, Jin Yang, Yang Xiang, Hanqiu Wang, Li Li, Rongqing Zhang, Bo Tu, and Xiangqun Chen.  
 632 Trajbert: Bert-based trajectory recovery with spatial-temporal refinement for implicit sparse  
 633 trajectories. *IEEE Transactions on Mobile Computing*, 23(5):4849–4860, 2023.

634 Chandan Singh, Jeevana Priya Inala, Michel Galley, Rich Caruana, and Jianfeng Gao. Rethinking  
 635 interpretability in the era of large language models. *arXiv preprint arXiv:2402.01761*, 2024.

637 Chaoming Song, Tal Koren, Pu Wang, and Albert-László Barabási. Modelling the scaling properties  
 638 of human mobility. *Nature physics*, 6(10):818–823, 2010.

639 Jiawei Wang, Renhe Jiang, Chuang Yang, Zengqing Wu, Makoto Onizuka, Ryosuke Shibasaki,  
 640 Noboru Koshizuka, and Chuan Xiao. Large language models as urban residents: An llm agent  
 641 framework for personal mobility generation. *Advances in Neural Information Processing Systems*,  
 642 37:124547–124574, 2024.

643 Xinhua Wu, Haoyu He, Yanchao Wang, and Qi Wang. Pretrained mobility transformer: A founda-  
 644 tion model for human mobility. *arXiv preprint arXiv:2406.02578*, 2024.

645 An Yang, Anfeng Li, Baosong Yang, Beichen Zhang, Binyuan Hui, Bo Zheng, Bowen Yu,  
 646 Chang Gao, Chengan Huang, Chenxu Lv, et al. Qwen3 technical report. *arXiv preprint  
 647 arXiv:2505.09388*, 2025.

648 Song Yang, Jiamou Liu, and Kaiqi Zhao. Getnext: Trajectory flow map enhanced transformer for  
 649 next poi recommendation. In *Proceedings of the 45th International ACM SIGIR Conference on*  
 650 *research and development in information retrieval*, pp. 1144–1153, 2022.

651 Yuan Yuan, Huandong Wang, Jingtao Ding, Depeng Jin, and Yong Li. Learning to simulate daily  
 652 activities via modeling dynamic human needs. In *Proceedings of the ACM Web Conference 2023*,  
 653 pp. 906–916, 2023.

654 Yuan Yuan, Jingtao Ding, Depeng Jin, and Yong Li. Learning the complexity of urban mobility with  
 655 deep generative network. *PNAS nexus*, 4(5):pgaff081, 2025.

656 Yanzhao Zhang, Mingxin Li, Dingkun Long, Xin Zhang, Huan Lin, Baosong Yang, Pengjun Xie,  
 657 An Yang, Dayiheng Liu, Junyang Lin, et al. Qwen3 embedding: Advancing text embedding and  
 658 reranking through foundation models. *arXiv preprint arXiv:2506.05176*, 2025.

659 Zhen Zhou, Ziyuan Gu, Xiaobo Qu, Pan Liu, Zhiyuan Liu, and Wenwu Yu. Urban mobility foun-  
 660 dation model: A literature review and hierarchical perspective. *Transportation Research Part E:*  
 661 *Logistics and Transportation Review*, 192:103795, 2024.

662 Yuanshao Zhu, Yongchao Ye, Shiyao Zhang, Xiangyu Zhao, and James Yu. Difftraj: Generating  
 663 gps trajectory with diffusion probabilistic model. *Advances in Neural Information Processing*  
 664 *Systems*, 36:65168–65188, 2023.

665 Yuanshao Zhu, James Jianqiao Yu, Xiangyu Zhao, Qidong Liu, Yongchao Ye, Wei Chen, Zijian  
 666 Zhang, Xuetao Wei, and Yuxuan Liang. Controltraj: Controllable trajectory generation with  
 667 topology-constrained diffusion model. In *Proceedings of the 30th ACM SIGKDD Conference on*  
 668 *Knowledge Discovery and Data Mining*, pp. 4676–4687, 2024a.

669 Yuanshao Zhu, James Jianqiao Yu, Xiangyu Zhao, Xuetao Wei, and Yuxuan Liang. Unitraj: Learn-  
 670 ing a universal trajectory foundation model from billion-scale worldwide traces. *arXiv preprint*  
 671 *arXiv:2411.03859*, 2024b.

672

## 673 A USE OF LLMs

674 We used LLMs to assist in writing the paper, such as identifying typos and correcting grammatical  
 675 errors, as well as polishing some paragraphs.

## 676 B SEMANTIC INFORMATION DESCRIPTION

### 677 Semantic Information Example

- 678 • **Location Address:** The location is situated at South Street, Hapeville, 30354, United States.
- 679 • **Geographic Coordinates and Boundary:** The center of the location is at **latitude 33.6544382**  
 680 and **longitude -84.4045157**. The area is bounded by:
  - 681 – **Minimum latitude:** 33.654528
  - 682 – **Maximum latitude:** 33.6548927
  - 683 – **Minimum longitude:** -84.403952
  - 684 – **Maximum longitude:** -84.4036685
- 685 • **OpenStreetMap (OSM) Details:**
  - 686 – **OSM Type:** way
  - 687 – **OSM ID:** 975678110
  - 688 – **Place ID:** 132886
- 689 • **Points of Interest (POIs):** The location includes 1 fast food, 1 restaurant.
- 690 **POI Categories:** "gid", "finance", "public", "transport", "entertainment", "health", "service", "ed-  
 691 ucation", "government", "religion", "accommodation", "food", "cafe", "fast\_food", "ice\_cream",  
 692 "pub", "restaurant", "shop\_beauty", "shop\_clothes", "boutique", "shop\_transport", "retail", "com-  
 693 modity", "marketplace", "home-improvement", "sport", "public\_transport", "kindergarten", "office",  
 694 "recycling", "travel\_agency", "tourism", "shop\_livelihood", "residential", "dormitory".

702 **C DATASET DETAILS**  
 703

704 **Dataset Statistics** The statistical overview of the datasets used is presented in Table 8.  
 705

706  
 707 **Table 8: Statistical information for the trajectory datasets used in our experiments.**

708 <b>City</b>	709 <b>Duration</b>	710 <b>Locations</b>	711 <b>Trajectories</b>
710 Atlanta	7 days	711 1,175	712 200,000
711 Chicago	7 days	712 4,166	713 200,000
712 Seattle	7 days	713 1,046	714 200,000
713 Washington	7 days	714 1,361	715 200,000

716 **D TASK PROMPT EXAMPLES**  
 717

718 **Geographic Location Understanding:**

719  
 720 • **loc2id:** Your task is to infer the corresponding Location index based on the geographic location  
 721 information: [location]\n Its Location index is :  
 722 • **id2loc:** Your goal is to learn and remember the geographic location information represented by  
 723 the Location index.\n The geographic information of Location index [index] is :

724 **Understanding + Prediction:**  
 725

726 This is a user trajectory prediction task. Your goal is to predict the next location index using  
 727 both an authoritative trajectory text and a possibly noisy sequence embedding.

728 **Provided:**

- Ground-truth trajectory text (always correct): <traj\_data>
- Sequence embedding of the trajectory (auxiliary signal): <sequence>

729 **Conflict/irrelevance handling:**

- If any embedding-based interpretation contradicts the trajectory text or reflects a trajectory largely unrelated to the text, disregard the embedding interpretation and rely on the text.
- Only incorporate embedding cues that align with the text.

730 **Tasks:**

1. Based on the trajectory text and your analysis of the sequence embedding (ignore it if inconsistent with the text), produce the user's spatio-temporal trajectory features, filling the template exactly:

731 *Summary of the spatio-temporal trajectory features:*

- *Most frequently visited locations (visited more than once): [Output at most the first three (if any)]*
- *Probability of visits by time period (rounded to 5%): [list all periods with probability values, even if 0%]*

2. Using these features and the inputs(if sequence embedding appears inconsistent with the textual trajectory, ignore it), predict the user's next location index.

745 Output only the completed feature block and the final prediction. Do not include explanations.  
 746

747 **Understanding + Generation:**  
 748

749 The user's original trajectory data contains weekday, timestamp, and location index information.  
 750 Below is the encoded vector of the user's trajectory sequence for the past two  
 751 days:  
 752

753 <sequence>  
 754

755 In addition, there also has a special text format description of the user's historical trajectory  
 756 as supplementary information: <history\_text>.

757 You need to first carefully interpret both the encoded trajectory sequence (embedding) and  
 758 the historical textual trajectory description, and then complete the following two tasks:

756  
 757     **Step 1:** Generate 'Summary of the trajectory preferences for this user' strictly in the fol-  
 758     lowing format:

759         *Summary of the trajectory preferences for this user:*

760         - *Most frequently visited locations (visited more than once): [Output at most the first three  
 761         (if any)]*

762         - *Probability of visits by time period (rounded to 5%): [list all periods with probability  
 763         values, even if 0%]*

764         - *Frequently visited locations during each time period: [list per period; if none, explicitly  
 765         say 'No location was visited more than once'].*

766     **Step 2:** Based on both the summary and the encoded vector together with the historical  
 767     textual trajectory description, generate the user's trajectory activity for the next day. Each  
 768     data point in the generated trajectory should be in the format: *At [time], visited location  
 769     [location index].*

770

771     **SELF-REFLECTION**

772  
 773     You are an intelligent assistant skilled at asking questions and thinking. Please solve  
 774     the following problem step by step. First, you should think through the reasoning pro-  
 775     cess and then provide the answer to the user. The reasoning process and answer are  
 776     contained in the <think> </think> and <answer> </answer> tags, respectively,  
 777     i.e., <think>reasoning process here </think><answer>answer here  
 778     </answer>.

779     You need to complete the following trajectory modification task:

780     **Input:**

781     Completely known input:

- 782         1. Given two days of historical behavior data
- 783         2. Previously generated user trajectory data for the next day
- 784         3. Statistical spatiotemporal features of historical behavior data
- 785         4. Statistical spatiotemporal features of real data for the next day
- 786         5. Given Modification Steps: [constraint], and then K trajectory modifications (the  
 787         specific value of K is determined by your own analysis).

788  
 789     **Task Requirements:** Based on fully known inputs, modify and improve previously gen-  
 790     erated trajectory data for the next day, using the given modification steps, and ensure that  
 791     the modified trajectory data is maximally consistent with the Statistical spatiotemporal fea-  
 792     tures of real data for the next day. The analytical support should only be derived from  
 793     fully known inputs. The final output should include a summary of the modification steps  
 794     and the corresponding reasons, as well as the final user trajectory for the next day after  
 795     the modification steps. Be careful not to analyze <a\_x><b\_x><b\_x><d\_x> separately.  
 796     <a\_x><b\_x><b\_x><d\_x> together form a whole to describe a specific location. Do  
 797     not add or generate new <a\_x><b\_x><b\_x><d\_x> when modifying. When modifying  
 798     a previous future trajectory, only locations that have appeared in history and previously  
 799     generated future trajectories, as well as locations that have appeared in the spatiotemporal  
 800     features corresponding to the given future day's real trajectory data, can be used. For the  
 801     time modification, you can generate timestamps that are not in the historical sequence or  
 802     previously generated future tracks. Note that deleting a track, adding a track, or modifying  
 803     a track (either location, time, or both) is considered a single operation. Please complete the  
 804     reasoning analysis based on this, using as few modification steps as possible.

805     **Specific input data is as follows:**

806     Fully known input:

- 807         1. Given historical behavior data: [data1]
- 808         2. Previously generated user trajectory data for the next day: [data2]
- 809         3. Statistical spatiotemporal features of historical behavior data: [data3]
- 810         4. Statistical spatiotemporal features of real data for the next day: [data4]

810 E EVALUATION METRICS  
811812 PREDICTION TASK  
813814 The Hit Rate (or Accuracy) measures the proportion of correctly predicted next locations within the  
815 top- $k$  recommendations. The formula is:

816 Hit Rate@ $k$  =  $\frac{1}{|U|} \sum_{u \in U} \mathbb{I}(\text{rank}_u \leq k)$  (9)  
817  
818

819 where  $|U|$  is the total number of users, and  $\mathbb{I}(\cdot)$  is an indicator function that is 1 if the true next  
820 location is within the top- $k$  predictions, and 0 otherwise.  
821822 GENERATION TASK  
823824 **Bilingual Evaluation Understudy (BLEU):** A metric for evaluating the quality of generated text  
825 against a reference.

826 BLEU = BP · exp  $\left( \sum_{n=1}^N w_n \log p_n \right)$  (10)  
827  
828

829 where  $\text{BP} = \min(1, e^{1-r/c})$  is the brevity penalty,  $p_n$  is the modified  $n$ -gram precision,  $r$  is the  
830 reference length, and  $c$  is the candidate length.  
831832 **Total Variation Distance (TVD):** Measures the distance between two probability distributions.  
833

834  $\text{TVD}(P, Q) = \frac{1}{2} \sum_{i=1}^k |P(i) - Q(i)|$  (11)  
835

836 where  $P$  and  $Q$  are probability distributions over  $k$  classes,  $P(i)$  is the predicted probability of class  
837  $i$ , and  $Q(i)$  is the ground truth probability.  
838839 **Jensen-Shannon Divergence (JSD):** A smoothed and symmetric measure of the similarity be-  
840 tween two probability distributions.

841  $\text{JSD}(P\|Q) = \sqrt{\frac{1}{2}D_{\text{KL}}(P\|M) + \frac{1}{2}D_{\text{KL}}(Q\|M)}$  (12)  
842  
843

844 where  $M = \frac{1}{2}(P + Q)$  is the midpoint distribution, and  $D_{\text{KL}}$  is the Kullback-Leibler divergence:  
845

846  $D_{\text{KL}}(P\|Q) = \sum_{i=1}^k P(i) \log \frac{P(i)}{Q(i)}$  (13)  
847  
848

849 GENERATING INDICATOR ALGORITHMS  
850851 Our time data is granular with half-hourly intervals. We calculate JSD in half-hourly buckets, while  
852 TVD and BLEU are implemented using standard algorithm libraries such as `scipy` and `nltk`.  
853854 F BASELINE DETAILS  
855856 Our baseline selection spans different methodological families to ensure a comprehensive evalua-  
857 tion. Below is a brief introduction to the core principle of each selected model.  
858859 PREDICTION BASELINES  
860861 • **DeepMove** (Feng et al., 2018) is an attentional recurrent neural network that captures both long-  
862 term periodic patterns and short-term sequential regularities in user mobility.  
863 • **TrajBert** (Si et al., 2023) adapts the powerful BERT architecture to model trajectories by treating  
locations as tokens and learning deep, bidirectional contextual representations for prediction.

- **GETNext** (Yang et al., 2022) integrates a graph neural network to explicitly learn spatial relationships between locations with a Transformer-based encoder to capture complex spatio-temporal dependencies.
- **TrajFM** (Lin et al., 2024) is a foundation model for trajectories that is pre-trained on a massive dataset to learn universal mobility patterns adaptable to various downstream tasks.
- **Unitraj** (Zhu et al., 2024b) is a universal pre-trained model that unifies the representation of diverse trajectory data types, including spatio-temporal points, semantic texts, and graph structures.
- **TrajMoE** (Han et al., 2025) employs a Mixture-of-Experts (MoE) architecture where different "expert" sub-networks specialize in modeling distinct mobility patterns for more accurate and robust predictions.
- **Mobility-LLM** (Gong et al., 2024) is a large language model-based framework that reformulates trajectory prediction as a language modeling task by converting mobility data into textual sequences.
- **QT-Mob** (Chen et al., 2025) enhances LLMs for mobility prediction by incorporating a query-time adaptation mechanism that retrieves and integrates relevant external spatio-temporal knowledge at the time of inference.

## GENERATION BASELINES

- **DiffTraj** (Zhu et al., 2023) applies a denoising diffusion probabilistic model to generate realistic and diverse human trajectories by progressively refining a random noise signal into a structured sequence.
- **Marionette** (Deng et al., 2025) is a controllable trajectory generation model based on guided diffusion, allowing for the synthesis of trajectories that adhere to specific user-defined constraints or conditions.
- **COPB** (Shao et al., 2024a) leverages the Chain-of-Thought prompting technique with large language models to iteratively reason about user preferences and construct plausible, context-aware trajectories.
- **LLMob** (Wang et al., 2024) is a comprehensive framework that utilizes the generative and reasoning capabilities of large language models to produce human-like trajectories based on user profiles and historical data.

## G IMPLEMENTATION DETAILS

This experiment used four NVIDIA A800 40GB GPUs. We chose Qwen2.5-7B (Hui et al., 2024) as the backbone network. The experiments used the AdamW optimizer, with a cosine annealing learning rate and a warmup ratio of 0.03. The maximum learning rate for the cosine annealing algorithm was set to 1e-4, and both the minimum warmup learning rate and the initial warmup learning rate were set to 2e-5. We performed LoRA (Hu et al., 2022) fine-tuning and parallel training acceleration. All experiments were conducted with a maximum of 5 training epochs and a batch size of 96, and the best-performing model on the validation set was selected for testing. For the reflective inference experiments, we additionally used two NVIDIA A100 80G GPUs and chose Qwen3-4B (Yang et al., 2025) as the backbone network. Due to limited computing resources, we fixed the random seed to 42 and ran the experiment only once. For information on the model parameters involved in the method, please refer to the appendix below H.

## H MODEL CONFIGURATIONS

**Codebook Model:** The trajectory discretization is performed by a vector quantization model. Its encoder is an MLP with hidden layer dimensions of [2048, 1024, 512, 256, 128, 64]. The model utilizes four separate codebooks, each containing 512 embeddings of 64 dimensions. For training, we used the AdamW optimizer with a learning rate of  $1 \times 10^{-3}$  and a batch size of 1024.

**Mobility Foundation Model:** Our mobility foundation model is a Transformer-based architecture. It is configured with 4 layers, 4 attention heads, and an embedding dimension of 512. The model

918 was trained for 50 epochs using a learning rate of  $3 \times 10^{-4}$  and a batch size of 8 to process trajectory  
 919 sequences with a maximum length of 145.  
 920

921 **Large Language Model Fine-Tuning:** For the supervised fine-tuning (SFT) phase, we employed  
 922 the **Qwen2.5-7B** model. Due to computational constraints during the subsequent Generative Re-  
 923 jective Policy Optimization (GRPO) stage, we trained an auxiliary **Qwen3-4B** model. This smaller  
 924 model was tasked with the self-reflection and reasoning steps, enabling us to effectively complete  
 925 the GRPO training on the primary 7B model within our resource limits.  
 926

## 927 I CROWD FILTERING CRITERIA

929 **Late-night Commuters:** We define **Late-night Commuters** as individuals who undertake trips  
 930 between 10 PM and 6 AM. The specific criterion for this classification is that a user’s trips within this  
 931 time frame must account for more than three-quarters (75%) of their total daily trips. Trajectories  
 932 belonging to this user group were specially flagged to analyze their distinct mobility patterns.  
 933

934 **Users with Temporary Travel Plans:** To isolate and analyze non-habitual or temporary travel  
 935 behaviors, we established criteria to identify users with transient travel intentions. Our methodology  
 936 involves an examination of the top three most frequently visited locations within a user’s historical  
 937 and future trajectories.  
 938

- 939 • **Identification of New Plans:** If a location that is not among a user’s three most historically  
 940 frequent locations appears in their future trajectory, we classify this as the user having made  
 941 a new plan to visit a previously infrequently visited location.  
 942
- 943 • **Identification of Canceled Plans:** Conversely, if a location that ranks among the top three  
 944 most visited places in a user’s historical trajectory does not appear in their planned future  
 945 trajectory, we infer that the user has canceled a previously planned visit to a frequented  
 946 location.  
 947

948 **Weekend Users:** We constructed a specific data subset where the historical series contains trajectory  
 949 data from Thursday and Friday, which is then used to predict the user’s trajectory on Saturday.  
 950 Consequently, only users with complete and valid trajectory data for the preceding two days were  
 951 included in this predictive task.  
 952

## 953 J VISUALIZATION OF GENERATED TRAJECTORIES

954 We visualized the temporal and location distributions of trajectories generated by representative  
 955 algorithms under unconditional generation. As shown in Figure 2, compared to the baseline, the  
 956 trajectories generated by our method are much closer to the distribution of true trajectories. In par-  
 957 ticular, for location distribution, our method shows significant improvements in both high-frequency  
 958 and long-tail regions, demonstrating a higher fidelity to real-world mobility patterns.  
 959

972  
 973  
 974  
 975  
 976  
 977  
 978  
 979  
 980  
 981  
 982  
 983  
 984  
 985  
 986  
 987  
 988  
 989  
 990  
 991  
 992  
 993  
 994  
 995  
 996  
 997  
 998  
 999  
 1000  
 1001  
 1002  
 1003  
 1004  
 1005  
 1006  
 1007  
 1008  
 1009  
 1010  
 1011  
 1012  
 1013  
 1014  
 1015  
 1016  
 1017  
 1018  
 1019  
 1020  
 1021  
 1022  
 1023  
 1024  
 1025

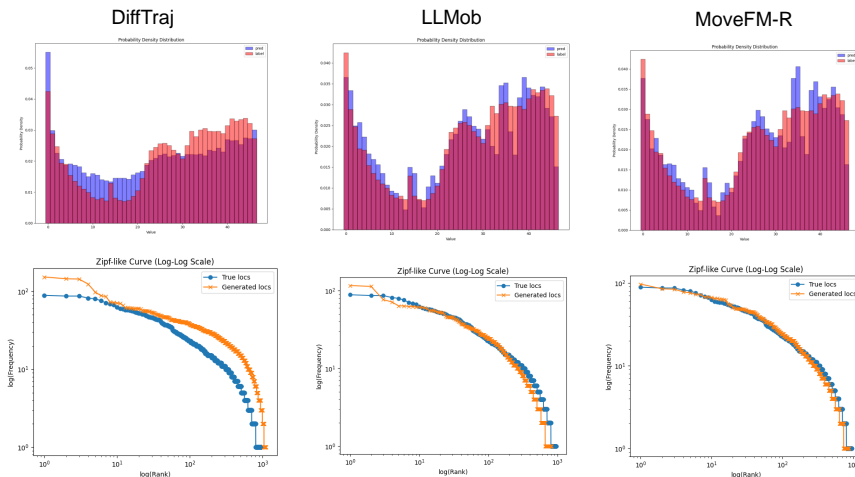


Figure 2: **Comparison of Temporal and Location Distributions.** We evaluate the distributions of generated trajectories from our model (MoveFM-R) against baselines (DiffTraj, LLMob). **Top row:** Visualization of the temporal distribution. The generated distribution (red) from our model more accurately matches the true temporal distribution (blue) of user activities over time. **Bottom row:** Visualization of the location distribution on a log-log scale (Zipf-like plot). The curve for our generated data (orange) shows a much tighter fit to the ground-truth data (blue) across the entire spectrum, from popular (head) to rare (tail) locations.